

Structural, magnetic, and dielectric properties of Ni-Zn ferrite and Bi_2O_3 nanocomposites prepared by the sol-gel method

Jinmiao Han(韩晋苗), Li Sun(孙礼), Ensi Cao(曹恩思), Wentao Hao(郝文涛), Yongjia Zhang(张雍家), and Lin Ju(鞠林)

Citation: Chin. Phys. B, 2021, 30 (**9**): 096102. DOI: 10.1088/1674-1056/ac0904
Journal homepage: http://cpb.iphy.ac.cn; http://iopscience.iop.org/cpb

What follows is a list of articles you may be interested in

Structural, magnetic, and dielectric properties of Ni-Zn ferrite and Bi_2O_3 nanocomposites prepared by the sol-gel method

Jinmiao Han(韩晋苗), Li Sun(孙礼), Ensi Cao(曹恩思), Wentao Hao(郝文涛), Yongjia Zhang(张雍家), and Lin Ju(鞠林)
Chin. Phys. B, 2021, 30 (**9**): 096102. DOI: 10.1088/1674-1056/ac0904

Magnetoelectric coupling effect of polarization regulation in $BiFeO_3/LaTiO_3$ heterostructures

Chao Jin(金超), Feng-Zhu Ren(任凤竹), Wei Sun(孙伟), Jing-Yu Li(李静玉), Bing Wang(王冰), and Qin-Fen Gu(顾勤奋)
Chin. Phys. B, 2021, 30 (**7**): 076105. DOI: 10.1088/1674-1056/abf924

Effects of 3d-transition metal doping on the electronic and magnetic properties of one-dimensional diamond nanothread

Zhenzhen Miao(苗珍珍), Can Cao(曹粲), Bei Zhang(张蓓), Haiming Duan(段海明), Mengqiu Long(龙孟秋)
Chin. Phys. B, 2020, 29 (**6**): 066101. DOI: 10.1088/1674-1056/ab84dd

Magnetic properties of La_2CuMnO_6 double perovskite ceramic investigated by Monte Carlo simulations

S Mtougui, I EL Housni, N EL Mekkaoui, S Ziti, S Idrissi, H Labrim, R Khalladi, L Bahmad
Chin. Phys. B, 2020, 29 (**5**): 056101. DOI: 10.1088/1674-1056/ab7d95

Study on superstructure in ion co-doped $BiFeO_3$ by using transmission electron microscopy

Pu Shi-Zhou, Guo Chao, Li Mei-Ya, Chen Zhen-Lian, Zou Hua-Min
Chin. Phys. B, 2015, 24 (**4**): 046101. DOI: 10.1088/1674-1056/24/4/046101

Structural, magnetic, and dielectric properties of Ni–Zn ferrite and Bi_2O_3 nanocomposites prepared by the sol-gel method*

Jinmiao Han(韩晋苗)[1], Li Sun(孙礼)[1,†], Ensi Cao(曹恩思)[1], Wentao Hao(郝文涛)[1], Yongjia Zhang(张雍家)[1], and Lin Ju(鞠林)[2]

[1] College of Physics and Optoelectronics, Taiyuan University of Technology, Taiyuan 030024, China
[2] College of Physics and Electrical Engineering, Anyang Normal University, Anyang 455000, China

(Received 30 April 2021; revised manuscript received 2 June 2021; accepted manuscript online 8 June 2021)

Ni–Zn ferrite and Bi_2O_3 composites were developed by the sol-gel method. The structural, magnetic, and dielectric properties were studied for all the prepared samples. X-ray diffraction (XRD) was performed to study the crystal structure. The results of field emission scanning electron microscopy (FE-SEM) showed that the addition of Bi_2O_3 can increase the grain size of the Ni–Zn ferrite. Magnetic properties were analyzed by a hysteresis loop test and it was found that the saturation magnetization and coercivity decreased with the increase of Bi_2O_3 ratio. In addition, the dielectric properties of the Ni–Zn ferrite were also improved with the addition of Bi_2O_3.

Keywords: Ni–Zn ferrite, Bi_2O_3, magnetic properties, nanocomposites

PACS: 61.46.–w, 75.75.–c **DOI:** 10.1088/1674-1056/ac0904

1. Introduction

Ferrite is a kind of material with great research value, which possesses a few good magnetic properties, namely, high electric resistivity, low coercivity, and negligible eddy current loss for high frequency electromagnetic wave propagation.[1–6] Therefore, a ferrite is suitable for making high-frequency weak current electromagnetic devices, such as filters, loud speakers, and so on.[1]

The chemical formula of a spinel ferrite is MFe_2O_4 (such as $NiFe_2O_4$), which adopts the face-centered cubic crystal and each crystal cell contains eight molecular formulas.[3,7] In the spinel structure, oxygen ions are arranged approximately in a cubic close packing. Meanwhile, besides containing 32 oxygen ions, there are 32 octahedral positions and 64 tetrahedral positions as well in the crystal cell, among which 16 octahedral positions (B sites) and 8 tetrahedral positions (A sites) are filled by specific cations.[2,8,9] Depending on the potential applications, ferrite materials could have tailored values of magnetic parameters including coercive field (H_c), threshold field and ferromagnetic resonance band.[3]

As we know, the magnetic properties and microstructures of Ni–Zn ferrites are highly sensitive to some factors involved in the fabrication process (e.g., sintering conditions, preparation method, and nature of the metal oxides including dopants and/or impurities).[2] Until now, in order to improve the physical properties of a nickel–zinc ferrite, researchers have been devoted to the study of nickel–zinc ferrites, among which the construction of the composite system or doping of nickel–zinc ferrites is the most extensive.[7,10–12]

Zhang *et al.* reported the dielectric, magnetic and magnetoelectric properties of $Ni_{0.5}Zn_{0.5}Fe_2O_4$–$Pb(Zr_{0.48}Ti_{0.52})O_3$ composite ceramics prepared by the solid-state reaction method. XRD and SEM results showed that high dense composite ceramics without any foreign phases were obtained. The properties of the samples sintered at 1120 °C and 1140 °C showed similar behaviors, including phases, microstructure and dielectric, magnetic and magnetoelectric properties. The ceramics showed excellent dielectric and magnetic properties, which were stable in a large frequency range.[10] Lin *et al.* prepared laminated $Ca(Zn_{1/3}Nb_{2/3})O_3$ (CZN)–$Ni_{0.8}Zn_{0.2}Fe_2O_4$ (NZO) composites using the conventional solid-state sintering method. With increasing the NZO concentration, the diffraction peaks of NZO phase become strengthened gradually. At a lower frequency, the permittivity and dielectric loss of the CZN–NZO composites increase with the increasing NZO ratio. All the samples showed excellent magneto-dielectric properties in a wide frequency range from 10 MHz to 1 GHz.[11] Hu *et al.* investigated the composition, structural and magnetic properties of Co-doped Ni–Zn ferrite, which was prepared by the solid-state method. Moreover, the saturation magnetization (M_s) increased with increasing Co substitution and reaches the maximum value 135.5 emu/g at $x = 0.05$.[12] Li *et al.* showed that structure and static magnetic properties of Ti-substituted Ni–Zn–Co ferrite thin films synthesized by the sol-gel process. The average grain size of Ti-substituted Ni–Zn–Co ferrite thin films increased with Ti substitution. The saturation magnetization gradually increased with the increase of Ti substitution when $x \leq 0.06$, and decreased when $x > 0.06$. Besides, the coercivity initially increased with the increase of Ti

*Project supported by the National Natural Science Foundation of China (Grant No. 11804006) and the Natural Science Foundation of Shanxi Province, China (Grant Nos. 201901D111126 and 201901D111117).

†Corresponding author. E-mail: sunlitut@163.com

© 2021 Chinese Physical Society and IOP Publishing Ltd

substitution when $x \leq 0.03$, and decreased when $x > 0.03$.[7]

In previous studies, Bi_2O_3 was used to improve the low-temperature densification of Ni–Cu–Zn ferrites,[13] since Bi_2O_3 could promote grain growth, enhance the density of the sample and reduce the porosity via liquid phase sintering. And Bi_2O_3 could segregate at the grain boundaries as a liquid phase layer. Moreover, the addition of moderate content of Bi_2O_3 can enhance the intensity of x-ray diffraction peaks of Bi-doped ferrites.[14] Gan *et al.* reported that ion substitution can adjust magnetic properties of M-type barium ferrite, while Bi_2O_3 aids can lower the sintering temperature and improve ferrite densification.[15] It is noteworthy that influences of Bi_2O_3 on microstructure and magnetic properties of MnZn ferrite have been studied by Yu *et al.* The results indicate that Bi_2O_3 promotes a solid-state reaction and grain growth, reduces porosity and enhances density. In the MnZn ferrite doped with 0.06% Bi_2O_3, the grains are most homogeneous, the pores are the least, the initial permeability and saturation magnetic induction are the maximal, but the coercivity is the minimal.[16] Gan *et al.* synthesized spinel $Mg_{0.6}Cd_{0.4}Co_{0.05}Fe_{1.95}O_4$ ferrite with Bi_2O_3 dopant by using the LTCC technique. The results indicated that densification sintering results in ultra-low dielectric loss $\tan\delta_\varepsilon$ and magnetic loss $\tan\delta_\mu$ ($\tan\delta_\varepsilon \approx 0.003$, $\tan\delta_\mu \approx 0.035$). In addition, the samples presented enhanced magnetic properties, such as high saturation magnetization (approximately 37.94 emu/g) and appropriate coercivity (approximately 60.5 Oe) at 940 °C.[17] Xu *et al.* synthesized Ni–Cu–Zn ferrites with Bi_2O_3–Nb_2O_5 composite additives. Ni–Cu–Zn ferrites with low coercivity ($H_c = 94.75$ A/m) was obtained when 0.25 wt% Nb_2O_5–0.50 wt% Bi_2O_3 was added. It is proved that the improvement of compactness can enhance magnetic properties even though grain growth was suppressed.[18] Therefore, we speculated that the combination of Bi_2O_3 and Ni–Zn ferrite materials can enhance the density and improve the magnetic and dielectric properties of a Ni–Zn ferrite.

In our current work, $Ni_{0.5}Zn_{0.5}Fe_2O_4$–x% Bi_2O_3 ($x = 0$, 2.5, 5) nanocomposites with different Bi_2O_3 molar ratios were prepared by the sol-gel method. The microstructure, magnetic and dielectric properties were investigated. And the dielectric and magnetic properties of Ni–Zn ferrite were found to be improved by the addition of Bi_2O_3. These results indicated that $Ni_{0.5}Zn_{0.5}Fe_2O_4$–x% Bi_2O_3 ($x = 0$, 2.5, 5) ferrites might be a potential candidate for high-density recording media applications.[19]

2. Experimental details

2.1. Fabrication

The mixing of Bi_2O_3 and $Ni_{0.5}Zn_{0.5}Fe_2O_4$ composites were prepared by the sol-gel auto-combustion method. The starting materials used were nickel nitrate hexahydrate [$Ni(NO_3)_2{\cdot}6H_2O$, 99%], zinc nitrate hexahydrate [$Zn(NO_3)_2{\cdot}6H_2O$, 99%], bismuth nitrate pentahydrate [$Bi(NO_3)_3{\cdot}5H_2O$, 99%], ferrite nitrate nonahydrate [$Fe(NO_3)_3{\cdot}9H_2O$, 99%], polyethylene glycol [PEG 2000] and citric acid ($C_6H_8O_7$, > 99.5%). The metal nitrates weighted in precision and citric acid were dissolved in a beaker using minimum amounts of deionized water, keeping the citric acid to the metal ion ratio of 1:1.2 to form an aqueous solution. Then, the PEG and the ammonia were added into the mixed solution until the pH value was adjusted to 7. The mixture was stirred constantly at 80 °C using a water bath to form a dry gel. To remove the organic matter, the resulting gel is heated to spontaneous combustion and ground to form a powder. Next, the removal of organics and nitrate components can be further achieved by calcining ferrite powder at 600 °C for 2 hours at a heating rate of 10 °C/min in a muffle furnace and subsequently cooled to room temperature at the same rate in the furnace. The calcined powder is thoroughly ground and then pressed at a pressure of 40 MPa to form pellets with a diameter of 10 mm and a thickness of 1.5 mm. These pellets were sintered at 1000 °C for 5 hours and then cooled to room temperature to get the final ferrite ceramics. The temperature ramps for sintering are 5 °C/min for heating and 10 °C/min for cooling to 200 °C, then cooling naturally to room temperature. In order to test the electrical properties, some samples were silvered.

2.2. Characterization

The x-ray diffraction (XRD) patterns of Ni–Zn ferrite and Bi_2O_3 composites were acquired using Cu K_α radiation on an Ultima IV diffractometer. The fractured cross-sectional microstructures were investigated with a JSM-7100F field emission scanning electronic microscope (FE-SEM). Magnetic behavior of samples was determined using a vibrating sample magnetometer (VSM, BKT-4600 with a 1.5 T electromagnet). The dielectric properties of the Ni–Zn ferrite and Bi_2O_3 composite samples deposited with silver were measured by an LCR meter Agilent E4980A with an oscillation voltage of 0.5 V over the frequency range from 20 Hz to 2 MHz.

3. Results and discussion

3.1. Structural properties

The crystal structure was determined by the XRD technique. Figure 1 shows the XRD patterns of composites samples of $Ni_{0.5}Zn_{0.5}Fe_2O_4$–x% Bi_2O_3 ($x = 0$, 2.5, 5) with different Bi_2O_3 molar ratio. It can be clearly seen that the sample has good crystallinity. All the diffraction peaks of $Ni_{0.5}Zn_{0.5}Fe_2O_4$ were well matched with the standard diffraction peaks of powder (JCPDS: 08-0234), and no other impurity peaks appeared, indicating that the prepared samples had good

spinel structure. When the $Ni_{0.5}Zn_{0.5}Fe_2O_4$ is combined with Bi_2O_3, the two substances can coexist well without other impurities, and the newly formed peaks still had a typical spinel structure. Also, all the crystal plane indexes of corresponding diffraction peaks were assigned in Fig. 1.

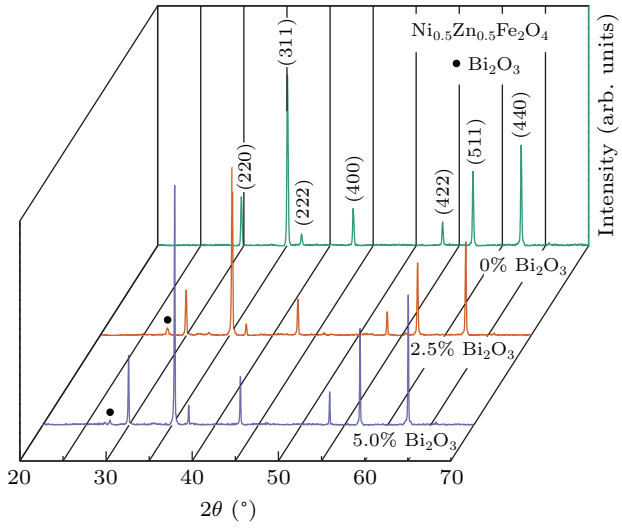


Fig. 1. XRD patterns of $Ni_{0.5}Zn_{0.5}Fe_2O_4$–x% Bi_2O_3 ($x = 0$, 2.5, 5) ceramic samples sintered at 1000 °C.

Figures 2(a)–2(c) shows the FE-SEM diagram of the cross section of the above samples and the mathematical statistical distribution of grain size obtained from the FE-SEM diagram (Figs. 2(d)–2(f)). It can be seen that the grain size distribution of all the samples is relatively uniform and the microstructure is relatively dense. The average grain size are respectively 0.26 μm, 0.28 μm and 0.50 μm with the increase of Bi_2O_3 content. It is obvious that the Bi_2O_3 is effective in the densification and enhancement of grain growth. When the molar ratio reaches 5%, the average grain size increases greatly, indicating that Bi_2O_3 and $Ni_{0.5}Zn_{0.5}Fe_2O_4$ combined well in this proportion. Bi_2O_3 is a low melting point substance with a melting point of 820 °C. In the sintering process of Ni–Zn ferrites and Bi_2O_3 composites, liquid phase will be formed, thus reducing the reflected activation energy and further promoting the growth of grains.[14]

Moreover, some researchers have shown that the ferrite ceramic samples containing Bi_2O_3 complex may form eutectic and deposit at grain boundary during sintering.[16] At the same time, the liquid phase formed by Bi_2O_3 will accelerate the diffusion and separation of ions in the reaction process. Grains grow larger and grain boundaries become more obvious, the porosity is easy to escape from the particles along the grain boundary, thus reducing the porosity.[16] The formation of Bi_2O_3 in the liquid phase can promote the growth of the grain size of the Ni–Zn ferrite and increase the density.[14,16]

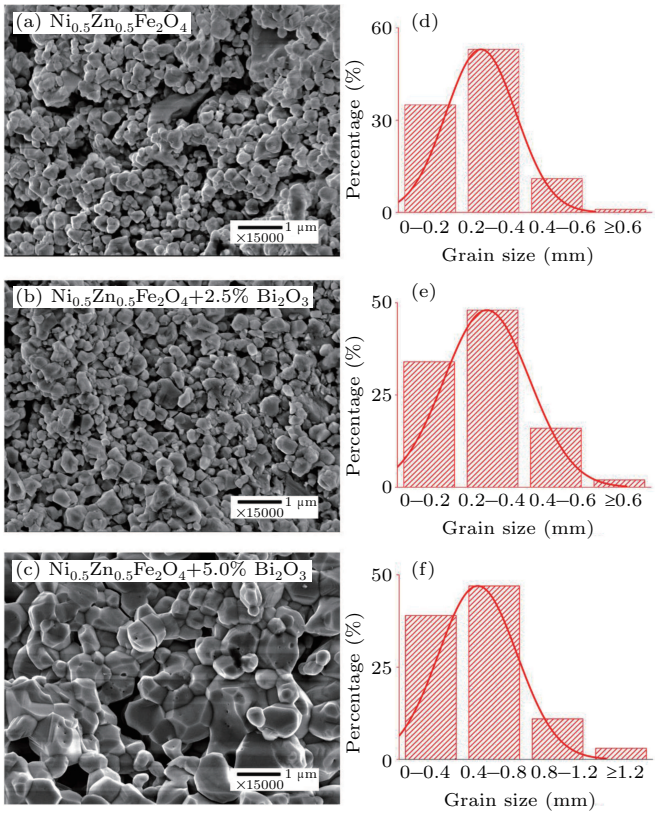


Fig. 2. FE-SEM micrographs of $Ni_{0.5}Zn_{0.5}Fe_2O_4$–x% Bi_2O_3 ($x = 0$ (a), $x = 2.5$ (b), $x = 5$ (c)). The graphs of (d)–(f) are histograms for grain size of $Ni_{0.5}Zn_{0.5}Fe_2O_4$–x% Bi_2O_3 samples ($x = 0$ (d), $x = 2.5$ (e), $x = 5$ (f)).

3.2. Magnetic properties

The room temperature magnetic hysteresis loops for different $Ni_{0.5}Zn_{0.5}Fe_2O_4$–x% Bi_2O_3 ($x = 0$, 2.5, 5) samples sintered at 1000 °C are displayed in Fig. 3. And Fig. 4 showed variation of M_s and H_c of composites samples of $Ni_{0.5}Zn_{0.5}Fe_2O_4$–x% Bi_2O_3 ($x = 0$, $x = 2.5$, $x = 5$) in different molar proportions sintered at 1000 °C. All the samples showed good magnetic properties of the ferrite. With the increase of x, the M_s and H_c of the sample decrease gradually. As seen, the addition of Bi_2O_3 has a noticeable effect on the magnetic properties of samples M_s dropped from 99.15 emu/g to 82.43 emu/g. And H_c descend from 82.08 Oe to 63.83 Oe. As discussed previously, with the increase of Bi_2O_3 content, the liquid phase reaction would be intensified, and the average grain size of the sample would increase gradually. It also means that Bi_2O_3 mainly segregates and concentrates in the grain boundary regions of Ni–Zn ferrites, and Bi_2O_3 would block the motion of the domain wall, which would cause the decrease of M_s.[16] In addition, the increase of non-magnetic Bi_2O_3 also weakens the magnetization, leading to the decrease of M_s.[20]

Similarly, the samples not combined with Bi_2O_3 show that the maximum value of H_c at 1000°C. It could be explained by the relation as follows:[21]

$$H_c = 3\left(kT_cK_1/aM_s\right)(1/D), \tag{1}$$

where K_1 is the first magneto crystalline anisotropy constant, T_c is Curie temperature, M_s is saturation magnetization, a is lattice constant and D is grain size. In this study, the rate of change of M_s is small, so it can be seen from the above equation that the average grain size is the main factor affecting the H_c value. H_c is inversely proportional to the grain size and a decrease in grain size increases H_c. A smaller grain size results in a high H_c due to pinning of domain walls by grain boundaries that requires a higher energy for switching.[22] Therefore, the addition of Bi_2O_3 will increase the H_c of the Ni–Zn ferrite.

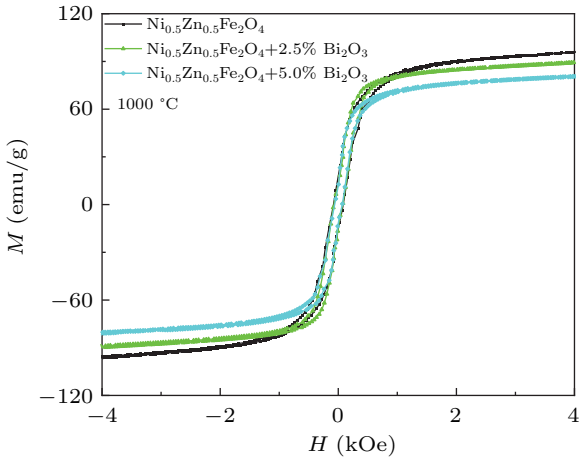


Fig. 3. The room temperature magnetic hysteresis loops for $Ni_{0.5}Zn_{0.5}Fe_2O_4$–x% Bi_2O_3 ($x = 0$, 2.5, 5) ceramic samples sintered at 1000 °C.

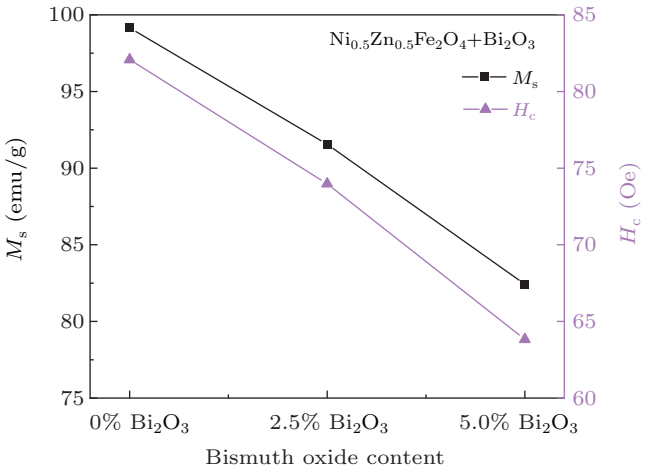


Fig. 4. Variation of M_s and H_c of $Ni_{0.5}Zn_{0.5}Fe_2O_4$–x% Bi_2O_3 ($x = 0$, 2.5, 5) ceramic samples sintered at 1000 °C.

3.3. Dielectric properties

Figure 5 shows the variation of a real dielectric constant (ε') and dissipation factor ($\tan\delta$) with frequency and temperature. It is obvious that ε' tends to decrease with increasing frequency between 20 Hz and 2 MHz. This is because in the hopping process of electrons, the accumulation of electrons in the grain boundary will lead to the increase of the grain boundary resistance, so the ε' value is small at high frequencies.[23] The value of dielectric constant increases with the increase of temperature. The results show that the dielectric properties of the ferrite can be improved effectively when the Bi_2O_3 is combined with nickel–zinc ferrite. Because the charge hopping is thermally activated process, dielectric polarization increases with increasing temperature resulting into an increase in dielectric constant.[24] The dielectric constant is usually affected by dipolar, electronic, ionic and interfacial polarizations.[25] And at high frequencies, electron polarization plays a major role, electronic contribution is weakly temperature dependent and is confirmed in Fig. 5.

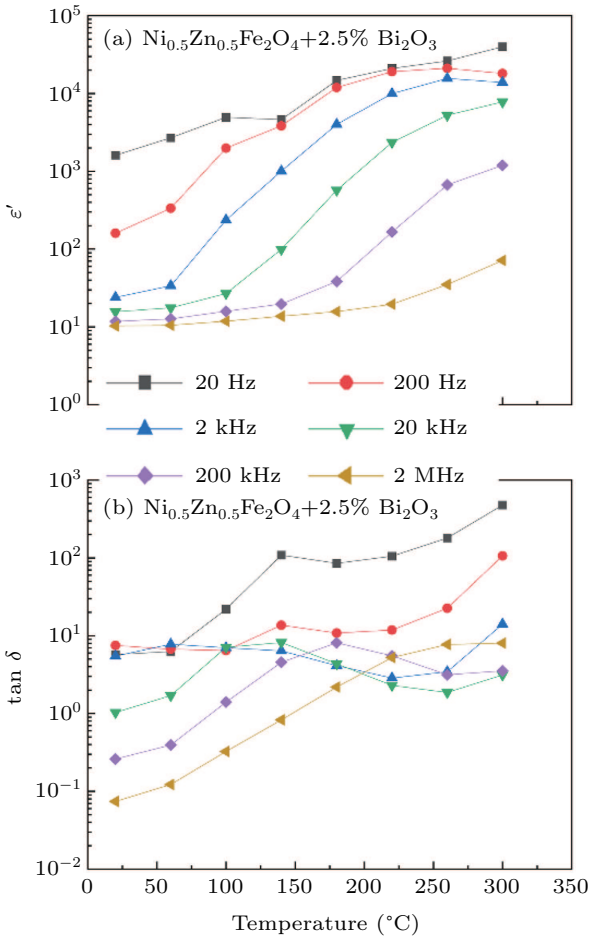


Fig. 5. Different temperature frequency dependence of ε' and $\tan\delta$ of the prepared $Ni_{0.5}Zn_{0.5}Fe_2O_4$–2.5%Bi_2O_3 ceramic samples.

Besides, it can be seen from the Fig. 5 that the $\tan\delta$ of different frequencies increases first and then decreases with the increase of temperature. As the frequency increases, $\tan\delta$ decreases gradually because at low frequencies, the application field frequency is equal to the hopping frequency of the current carrier. The hopping frequency is inconsistent with the applied frequency in the high frequency, which results the low $\tan\delta$.[26] And another reason for the lower $\tan\delta$ at high frequencies may be the suppression of domain wall motion.[27]

Figure 6 shows the variation of real dielectric constant (ε') and dissipation factor ($\tan\delta$) with frequency of $Ni_{0.5}Zn_{0.5}Fe_2O_4$–x% Bi_2O_3 ($x = 0$, 2.5, 5) ceramic sample. It is obvious that the relative dielectric constant of the sample increases with the increase of Bi_2O_3 content. Since Bi_2O_3 is

a kind of material with low melting temperature. It is easy to transform into liquid during the sintering process, and then flows to the grain boundary to help and support the grain growth, which makes the sample denser and lower porosity. As a result, the dielectric constant increases.[17]

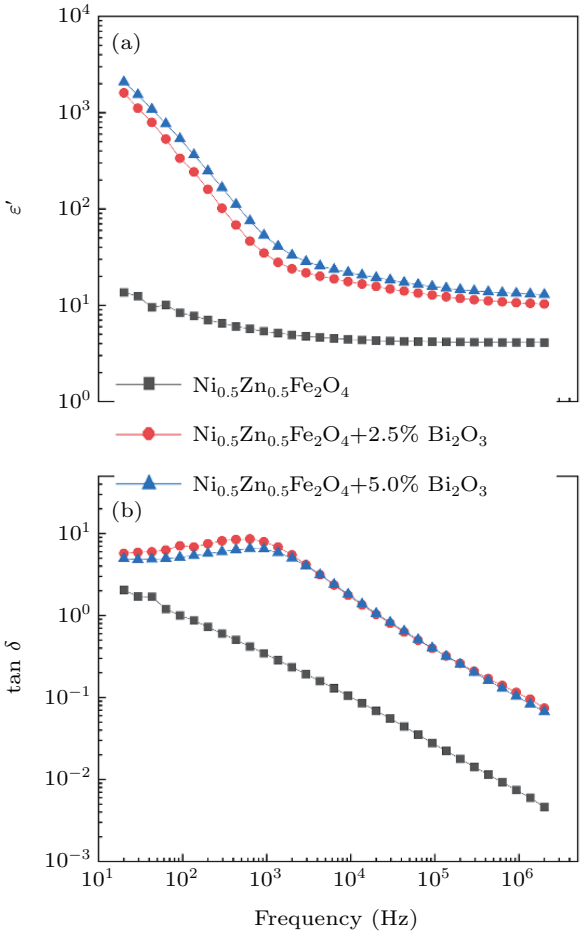


Fig. 6. Room temperature frequency dependence of ε' and $\tan\delta$ of the prepared $Ni_{0.5}Zn_{0.5}Fe_2O_4$–x% Bi_2O_3 ($x = 0$, 2.5, 5) ceramic samples.

Compared with pure ferrite, the ε' of the ferrite complex containing Bi_2O_3 increased significantly at low frequency, but decrease rapidly as frequency increases. In the high frequency region, the contribution of the orientation mechanism of the inherent electric moment to polarization decreases to zero due to the high molecular mass and high inertia.[28] With low mass and low inertia, the electron is able to keep up with the changes of high-frequency electric field. Thus, at high frequencies, only electron polarization is left, leading to a sharp drop in the dielectric constant. This phenomenon shows dielectric dispersion at lower frequencies which might be due to the interfacial polarization.[19] According to the double-layer dielectric model, polycrystalline spinel ferrite and composites have a two-layer structure called low resistivity grain boundary and high resistivity grain boundary.[29] In composites, the low conductivity grain is surrounded by the high resistivity grain boundary, so the composites will form a non-uniform structure.[29] Because the electrical conductivity of Bi_2O_3 and $Ni_{0.5}Zn_{0.5}Fe_2O_4$ is different, the two materials form an uneven double layer when they are combined. Due to the polyphase structure and non-uniform internal conduction of the composite material, the relative dielectric constant is relatively large in the low frequency region.[29] As can be seen from Fig. 6, the dielectric constant of the complex is larger at low frequencies. As the frequency gradually increases, ferrite ions will gradually aggregate at the grain boundary. Meanwhile, grain boundaries become more active and provide a rapid response at lower frequencies to the applied electric field, leading to high polarization and high resistivity grain boundary.[29] Therefore, a large number of ferrite ions accumulate at the grain boundary interface, resulting in a higher dielectric constant.[29] The dielectric constant of $Ni_{0.5}Zn_{0.5}Fe_2O_4$–Bi_2O_3 composites are relatively stable at the frequency of 10^5 Hz, which might be due to the inconsistency of electric dipole with the fast variation of electric field.[29] The $\tan\delta$ of the sample is shown in Fig. 6. In the low frequency region, the $\tan\delta$ of the sample is high, and with the increase of frequency, the $\tan\delta$ decreases gradually. In addition, ferrite composites containing Bi_2O_3 exhibit higher $\tan\delta$. This is because the space charge polarization in the low frequency band leads to high $\tan\delta$.[29] When the frequency increases, the frequency of the alternating electric field becomes faster, the charge accumulation decreases, and the $\tan\delta$ decreases.[29] A dielectric relaxation peak appears in $\tan\delta$–T curve (see Fig. 5(b)), which is due to the conduction in ferrite grain and grain boundaries.[29]

4. Conclusion

In this study, different $Ni_{0.5}Zn_{0.5}Fe_2O_4$–x%Bi_2O_3 ($x = 0$, 2.5, 5) samples were prepared by the sol-gel auto-combustion method. A small addition of Bi_2O_3 is a benefit for the grain growth but does not affect the spinel structure of the Ni–Zn ferrite. The dielectric properties of the composite materials are greatly improved in the low frequency region. From 200 Hz to 20 kHz, the temperature has a significant effect on the dielectric properties of the composite. The magnetic properties are also improved with the increase of Bi_2O_3 content.

References

[1] Venturini J, Wermuth T B, Machado M C, Arcaro S, Alves A K, Viegas A D and Bergmann C P 2019 *J. Eur. Ceram. Soc.* **39** 3442
[2] Kaur A and Bhargava G K 2021 *Mater. Today. Proc.* **37** 3082
[3] Jadhav J, Biswas S, Yadav A K, Jha S N and Bhattacharyya D 2017 *J. Alloys Compd.* **696** 28
[4] Golchinvafa S, Masoudpanah S M and Jazirehpour M 2019 *J. Alloys Compd.* **809** 151746
[5] Akyol M, Adanur İ, Ayaş A O, Karadağ F and Ekicibil A 2018 *J. Alloys Compd.* **744** 528
[6] Sharma A, Harvinderjeet and Harmanpreet 2021 *Mater. Today. Proc.* **37** 3058
[7] Li L, Wang R, Tu X and Peng L 2014 *J. Magn. Magn. Mater.* **355** 306
[8] Waghmare S P, Borikar D M and Rewatkar K G 2017 *Mater. Today. Proc.* **4** 11866

[9] Li L Z, Zhong X X, Wang R, Tu X Q and Peng L 2017 *J. Magn. Magn. Mater.* **433** 98
[10] Zhang Y, Zhou J P, Liu Q, Zhang S and Deng C Y 2014 *Ceram. Int.* **40** 5853
[11] Lin Y, Liu X, Yang H, Wang F and Liu C 2017 *Mater. Res. Bull.* **86** 101
[12] Hu J, Ma Y, Kan X, Liu C, Zhang X, Rao R, Wang M and Zheng G 2020 *J. Magn. Magn. Mater.* **513** 167200
[13] Wang S F, Wang Y R, Yang T C, Chen C F, Lu C H and Huang C Y 2000 *J. Magn. Magn. Mater.* **220** 129
[14] Sun K, Lan Z, Yu Z, Li L, Huang J and Zhao X 2008 *J. Phys. D: Appl. Phys.* **41** 235002
[15] Gan G, Zhang H, Li Q, Li J, Li M, Xu F and Jing Y 2018 *Mater. Res. Bull.* **97** 37
[16] Yu Z, Sun K, Li L, Liu Y, Lan Z and Zhang H 2008 *J. Magn. Magn. Mater.* **320** 919
[17] Gan G, Zhang D, Zhang Q, Wang G, Huang X, Yang Y, eRao Y, Li J, Xu F, Wang X, Chen R T and Zhang H 2019 *Ceram. Int.* **45** 12035
[18] Xu F, Zhang D, Wang G, Zhang H, Yang Y, Liao Y, Jin L, Rao Y, Li J, Xie F and Gan G 2019 *J. Alloys* **776** 954
[19] Junaid M, Khan M A, Hashmi Z M, Nasar G, Kattan N A and Laref A 2020 *J. Mol. Struct.* **1221** 128859
[20] Yang Y, Zhang H, Li J, Rao Y, Wang G and Gan G 2020 *Ceram. Int.* **46** 25697
[21] Kavanloui M and Hashemi B 2011 *Mater. Des.* **32** 4257
[22] Liu C, Lan, Z, Jiang X, Yu Z, Sun K, Li L and Liu P 2008 *J. Magn. Magn. Mater.* **320** 1335
[23] Ahmad Z, Atiq S, Abbas S K, Ramay S M, Riaz S and Naseem S 2016 *Ceram. Int.* **42** 18271
[24] Devan R S, Ma Y R and Chougule B K 2009 *Mater. Chem. Phys.* **115** 263
[25] Mohanty N K, Behera A K, Satpathy S K, Behera B and Nayak P 2015 *J. Rare Earths* **33** 639
[26] Tahir Farid H M, Ahmad I, Ali I, Mahmood A and Ramay S M 2018 *Eur. Phys. J. Plus* **133** 41
[27] Ghosh M P, Datta S, Sharma R, Tanbir K, Kar M and Mukherjee S 2021 *Mater. Sci. Eng. B* **263** 114864
[28] Batoo K M 2011 *J. Phys. Chem. Solids* **72** 1400
[29] Dagar S, Hooda A, Khasa S and Malik M 2019 *J. Alloys Compd.* **806** 737